International Journal of Innovative
Computing, Information and Control
Volume **14**, Number **6**, December **2018**

 ISSN 1349-4198
pp. **2273–2290**

PATH FOLLOWING CONTROLLER DESIGN FOR UNMANNED SURFACE VEHICLE BASED ON TRAJECTORY LINEARIZATION CONTROL

Bingbing Qiu, Guofeng Wang*, Yunsheng Fan, Dongdong Mu and Xiaojie Sun

School of Marine Electrical Engineering
Dalian Maritime University
No. 1, Linghai Road, Dalian 116026, P. R. China
{ bbqiu.dmu; ddmu.phd; xjsun.phd }@gmail.com; yunsheng@dlmu.edu.cn
*Corresponding author: gfwangsh@163.com

Received February 2018; revised June 2018

Abstract. *This paper develops a novel path following control strategy for the path following of underactuated unmanned surface vehicle (USV) under the unmodeled dynamics and external disturbances. The proposed controller is designed using trajectory linearization control and fuzzy disturbance observer (FDO). First, trajectory linearization control is introduced into the field of ship motion control, which is an effective control method for solving nonlinear tracking and system decoupling. Second, the nonlinear coordinate transformation is constructed to solve underactuated model problems, which will result in a "global design". Then, to enhance performance and robustness of the system, FDO is designed to estimate the unmodeled dynamics and external disturbances to achieve real-time online compensation, and robust control term can overcome the influence of approximation error. It is proved that all error signals in the system are uniformly ultimately bounded by Lyapunov functions. At last, comparisons and simulation results are presented to demonstrate the effectiveness of this proposed control strategy.*
Keywords: Underactuated USV, Trajectory linearization control, FDO, Path following

1. **Introduction.** With the rapid development of ocean techniques, USV becomes gradually to be a hotspot of research. USV is a kind of small surface movement platform, which not only has the advantages of being fast, small volume, low cost, but also it has the ability of autonomous navigation. Thus, USV has been widely used in many applications, such as ocean surveillance, search, rescue, and military [1]. In order to accomplish task accurately, the controller of a higher precision and strong anti-interference ability needs to be designed for USV. Therefore, there is a huge challenge and difficulty for controller design.

According to the different control targets, foreign scholars Encarnacao and Pascoal [2] divided ship motion control into three parts: point stabilization, trajectory tracking (TT) and path following (PF). The point stabilization can be regarded as the generation of control inputs to drive USV from any initial point to a target point [3]. TT aims at controlling USV to track a given time-varying trajectory [4]. In path following control scenario [5], USV is required to follow a path at a certain speed that is specified without temporal constraint. To contrast between TT and PF, the tracking error established by the latter is a function mapping relationship between the system state and the reference path, which is more robust to the system. PF is easier to implement than trajectory tracking and closer to practical engineering. Therefore, the study of PF has important academic value and

DOI: 10.24507/ijicic.14.06.2273

practical value. At present, a variety of control schemes associated with PF control design for surface vessel have been developed in literature. A guidance-based path following approach is proposed by Breivik and Fossen in [6], which makes autonomous underwater vehicles move along designated paths in a 3D ocean space. In [7], the global tracking problem for an underactuated ship is studied with only two propellers by Lyapunov's direct method. An adaptive neural network control strategy is presented in [8], where a fully actuated marine surface vessel with multiple output constraints is considered. In [9], the adaptive path following control algorithm is proposed by an identified dynamic model. Based on adaptive dynamic surface control and vehicles coordination, the distributed cooperative path following control of multi-robot systems is proposed in [10]. In [11], a navigation, guidance and control system are designed for environmental monitoring, and the sliding mode controller is utilized in [12,13]. However, in the aforementioned works, external disturbances are not considered. In practice, it may be difficult to navigate along a given path because there exist various external disturbances. In [14], neural network minimum parameter learning method is employed to compensate the uncertainties and time-varying external disturbances. In [15], an adaptive robust controller for path following of underactuated surface vessels is proposed based on hierarchical sliding mode method, which is robust to uncertain parameters and time-varying disturbances. Based on the vectorial back-stepping technique with disturbance observer, trajectory tracking robust control law is designed by estimation of uncertain time-variant disturbances in [16]. A practical adaptive neural control algorithm is proposed in [17], which solves the problem of robust adaptive path-following control for uncertain underactuated ship.

Trajectory linearization control (TLC) was developed by Professor J. Jim Zhu in 1990s. It is a nonlinear control method based on differential algebra theory, which combines nonlinear dynamic inversion and a linear time-varying feedback stabilization. It linearizes the system along a nominal trajectory, and then casts nonlinear tracking into a regulation problem for the tracking-error dynamics. Moreover, owing to the specific structure, it provides a certain extent of robust stability and can be capable of rejecting disturbance in nature. Therefore, TLC has been successfully applied to the controlling of missiles [18], vehicle flight [19], helicopter [20] and fixed-wing vehicle [21]. However, TLC has never been used in the field of ship motion control. Therefore, by using TLC method, we design a path following controller for the underactuated USV in this paper. However, in [22], TLC makes the closed-loop system obtain local exponential stability along the nominal trajectory by theoretical analysis. With the increase uncertainties of the system, the local exponential stability cannot make the TLC have enough anti-interference and robustness. Hence, the performance of TLC method is reduced or invalid. To enhance system robustness, various modified TLC strategies have been explored in [23-26]. The first attempt is to enhance TLC by applying adaptive neural network technique in [23]. The second methodology is estimating and compensating the disturbances by using observers [24-26]. To improve the performance of the whole system, a fuzzy disturbance observer (FDO) is proposed in this paper, which can approximate arbitrarily well a highly nonlinear system [27]. FDO is exploited to estimate the unavailable states for uncertain and compensate the influence of uncertain factor of the system.

In this paper, we develop a novel path following controller by TLC and FDO. Under the influence of the unmodeled dynamics and external disturbances, the underactuated USV can track a specific trajectory accurately. The main contributions of this note can be summarized as follows.

(1) TLC is a nonlinear tracking and decoupling control method, compared with other methods, which is more effective due to its simplicity and robustness. It is also first introduced into the field of ship motion control.

(2) The original TLC cannot be applied to the design of the underactuated USV controller. Therefore, output-redefinition is introduced to solve underactuated model problems, which is the equivalent transformation of the model by the coordinate transformation.

(3) Under the influence of the unmodeled dynamics and external disturbances, to enhance performance of the system, FDO is constructed to estimate the uncertainties of the system and compensate for it.

(4) Combined with the advantages of TLC and FDO, we develop a novel path following controller for the underactuated USV in this paper. Compared with TLC and nonlinear disturbance observer-trajectory linearization control (NDO-TLC), FDO-TLC has better control performance. Finally, the simulation results demonstrate the effectiveness and the robustness of the proposed method.

The paper is organized as follows. Section 2 introduces system model and preliminaries. In Section 3, a novel path following controller for underactuated USV is designed. In Section 4, the stability analysis of system is given. Simulation results and comparisons are considered in Section 5. Finally, some conclusions are made and future research directions are introduced.

2. System Model and Preliminaries.

2.1. Modeling of underactuated USV.

The USV tracking control consists of two parts: position control and course control. When the USV deviates the tracking line, position control refers to the control of transverse distance. Owing to that the control objective is sailing along the reference line trajectory, here we are most concerned about transverse distance y and course angle ψ, and not longitudinal distance x. Therefore, the schematic diagram of the USV tracking control system is shown in Figure 1.

In Figure 1, the heavy line and the dash line represent the set track line, the actual line of motion, respectively. (y, x) represents the position of USV in X_0OY_0 coordinate system, and U_n is the resultant speed of USV. When the underactuated USV tracks the reference straight-line path, it can be observed that there exists the corresponding relationship between the posture of USV and the set track line at a certain time. To simplify the problem, we assume that track line and longitudinal distance x (north direction)

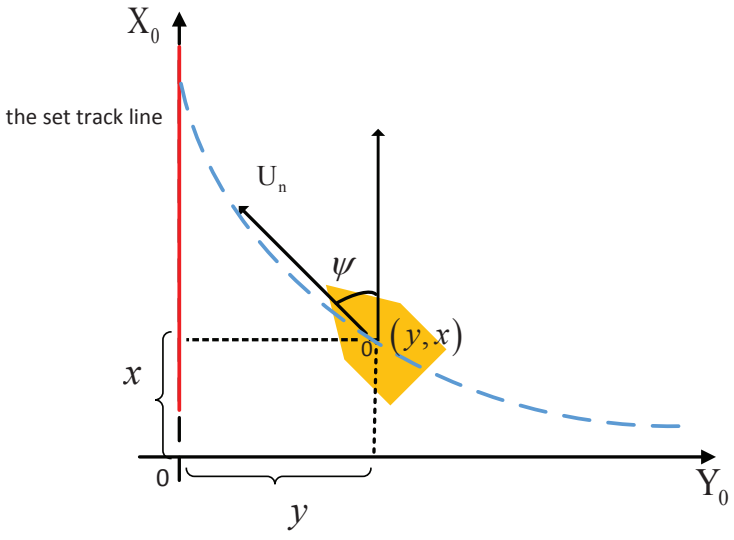

FIGURE 1. Coordinate diagram of the underactuated USV tracking control system

are coincident in this paper. Hence, heading angle is equal to course angle. Then the kinematic equation of planar motion [28] can be expressed as

$$\begin{cases} \dot{x} = \mu \cos\psi - v \sin\psi \\ \dot{y} = \mu \sin\psi + v \cos\psi \\ \dot{\psi} = r \end{cases} \tag{1}$$

where μ, v and r are surge velocity, sway velocity and yaw rate, respectively.

In the process of the USV control, due to the control effect of the closed-loop feedback, the change of the USV motion is close to the equilibrium state. At this time, the drift angle of USV is smaller, and the hydrodynamic is linear. Therefore, the mathematical model of the USV maneuvering can be properly simplified. We assume that the drift angle of USV can be ignored in this paper, then $\mu \gg 0$, $v \approx 0$. The resultant speed U_n of USV is the vector sum of μ and v, $U_n = \sqrt{\mu^2 + v^2} \approx \mu$. Here the mathematical model of USV can be simplified to

$$\begin{cases} \dot{x} = U_n \cos\psi \\ \dot{y} = U_n \sin\psi \\ \dot{\psi} = r \end{cases} \tag{2}$$

In practice, the linear motion of USV often presents unstable state or critical stability state. At this moment, the motion of USV is nonlinear. In addition, we have considered the influence of the nonlinear term in the system model. Thus, the nonlinear dynamic model [29] can be used in the model of course control in this paper, which is expressed as

$$\dot{r} = -\frac{1}{T} r - \frac{\alpha}{T} r^3 + \frac{K}{T} \delta \tag{3}$$

where δ is rudder angle, α is the coefficient of nonlinear model, and T, K are the performance indexes of USV maneuver.

From the above analysis, combining the systems (2) and (3), here longitudinal distance x is not considered. Finally, the nonlinear dynamic mathematical model of the USV linear track control system is obtained

$$\begin{cases} \dot{y} = U_n \sin\psi \\ \dot{\psi} = r \\ \dot{r} = -\dfrac{1}{T} r - \dfrac{\alpha}{T} r^3 + \dfrac{K}{T} \delta + \eta \\ y_1 = y \\ y_2 = \psi \end{cases} \tag{4}$$

where δ is the input of the system, y_1 and y_2 are the output of the system, and η is uncertainties of the system, respectively. Obviously, the system has obvious underactuated characteristics.

Control objective: Under the influence of the unmodeled dynamics and external disturbances, the position y and course angle ψ converge to target point (y_d, ψ_d) by the design of path following controller δ. In this paper, for simplicity, we define $y_d = 0$, $\psi_d = 0$.

2.2. **Nominal trajectory linearization method.** Consider the following multi-input multi-output (MIMO) nonlinear dynamic systems (without uncertainties)

$$\begin{cases} \dot{x} = f(x) + \sum\limits_{i=1}^{m} g_i(x) u_i \\ y_1 = h_1(x) \\ \quad \vdots \\ y_m = h_m(x) \end{cases} \tag{5}$$

where $x \in \mathbb{R}^n$, $u_i \in \mathbb{R}^n$ and $y_i \in \mathbb{R}^n$ are the system state, the input and output of the system, respectively. $f(x)$ is a fully smooth vector field of n-dimensional. $g_1(x), \ldots, g_m(x)$, $h_1(x), \ldots, h_m(x)$ are sufficiently smooth functions of states.

Define $u = [u_1, \ldots, u_m]^T$, $g(x) = [g_1(x), \ldots, g_m(x)]$, $h(x) = [h_1(x), \ldots, h_m(x)]^T$, $y = [y_1, \ldots, y_m]^T$, respectively. The system (5) can be expressed as

$$\begin{cases} \dot{x} = f(x) + g(x)u \\ y = h(x) \end{cases} \tag{6}$$

Let $\bar{x}$, $\bar{y}$, $\bar{u}$ be the nominal state, output, and control input, respectively. Then, the nominal trajectory satisfies

$$\begin{cases} \dot{\bar{x}} = f(\bar{x}) + g(\bar{x})\bar{u} \\ \bar{y} = h(\bar{x}) \end{cases} \tag{7}$$

Define the state tracking errors $e = x - \bar{x}$, output tracking errors $\Delta y = y - \bar{y}$ and control input tracking errors $\Delta u = u - \bar{u}$. The nonlinear tracking errors dynamics can be written as

$$\begin{cases} \dot{e} = f(\bar{x} + e) + g(\bar{x} + e)(\bar{u} + \Delta u) - f(\bar{x}) - g(\bar{x})\bar{u} = F(\bar{x}, \bar{u}, e, \Delta u) = F(t, e) \\ \Delta y = h(\bar{x} + e) - h(\bar{x}) = H(\bar{x}, e) = H(t, e) \end{cases} \tag{8}$$

By linearizing (8) along the nominal state and control $(\bar{x}, \bar{u})$, we obtain

$$\begin{cases} \dot{e} = A(t)e + B(t)\Delta u \\ \Delta y = C(t)e \end{cases} \tag{9}$$

where $A(t) = A(\bar{x}, \bar{u}) = \left(\frac{\partial f}{\partial x} + \frac{\partial g}{\partial x}u\right)\Big|_{\bar{x},\bar{u}}$, $B(t) = B(\bar{x}, \bar{u}) = g(x)\Big|_{\bar{x},\bar{u}}$, $C(t) = C(\bar{x}, \bar{u}) = \frac{\partial h}{\partial x}\Big|_{\bar{x},\bar{u}}$. The systems (8) and (9) satisfy the following assumptions.

Assumption 2.1. *Here $e(t) = 0$ is an isolated equilibrium point of the system (8), and $F : [0, \infty) \times D \to R^n$ can be continuously differentiable, among which $D = \{e \in R^n | \|e\| \leq R_e\}$. The Jacobian matrix $[\partial F / \partial e]$ is a bounded continuous function of t, which can meet the Lipschitz condition when D is satisfied [30].*

Assumption 2.2. *$(A(t), B(t))$ is uniformly completely controllable for the system (9).*

The linear time-varying feedback control law can be designed by the differential algebraic spectrum theory [31,32], which can be expressed as

$$\Delta u = u_{lc} = K(t)e \tag{10}$$

Here the system (6) is exponentially stable at the equilibrium point $e(t) = 0$, we define

$$A_c(t) = A(t) + B(t)K(t) \tag{11}$$

where $A_c(t)$ is Hurwitz, and it makes the system (9) asymptotically stable.

At present, the control rate of TLC can be expressed as

$$u = \bar{u} + u_{lc} \tag{12}$$

It is known that the state of the system (6) is local exponential stability along the nominal state trajectory. The TLC controller consists of two components, as shown in Figure 2.

(1) The pseudo dynamic inverse controller that generates the nominal control input (open-loop control) $\bar{u}$.

(2) The linear time-varying (LTV) feedback regulator (close-loop control) $u_{lc} = u(e)$ keeps the system stable and has certain response characteristics.

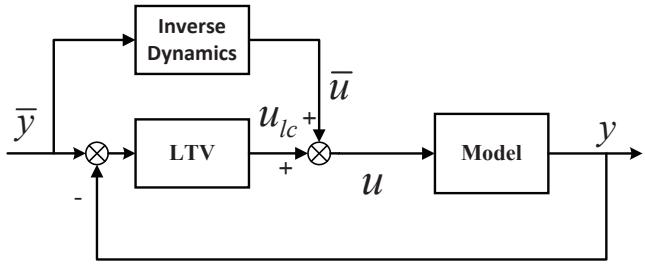

FIGURE 2. TLC scheme diagram

2.3. **Description of fuzzy logic systems.** A fuzzy system can approximate well a highly arbitrary nonlinear system, which consists of fuzzy IF-THEN rule, fuzzifier and fuzzy inference engine. The ith fuzzy rule is written as: If x_1 is A_1^i and x_n is A_n^i, then $\hat{\eta}$ is $\hat{\eta}^i$. Here $x = (x_1, x_2, \ldots, x_n)^T \in \mathbb{R}^n$ is the input vector, and $\hat{\eta} \in \mathbb{R}$ is the output variable. $A_1^i, A_2^i, \ldots, A_n^i$ are fuzzy variables and $\hat{\eta}^i$ is singleton fuzzifier. By using product inference, center-average and singleton fuzzifier, the output of the fuzzy system can be defined as

$$\hat{\eta}\left(x, \hat{\theta}\right) = \hat{\theta}^T \vartheta(x) \tag{13}$$

where $\hat{\theta}^T = \left[\hat{\eta}^1, \hat{\eta}^2, \ldots, \hat{\eta}^\varsigma\right]$ is adjustable parameter vector. $\vartheta^T(x) = \left[\vartheta^1(x), \vartheta^2(x), \ldots, \vartheta^\varsigma(x)\right]$ is fuzzy basis function vector, which can be expressed as

$$\vartheta^i(x) = \frac{\prod_{j=1}^{n} u_{A_j^i}(x_j)}{\sum_{i=1}^{\varsigma}\left(\prod_{j=1}^{n} u_{A_j^i}(x_j)\right)} \tag{14}$$

where $u_{A_j^i}(x_j)$ denotes the membership function of the fuzzy variable x_j, ς is the number of fuzzy rules and n is the number of input variables of the fuzzy system.

Assumption 2.3. *For any arbitrary $x \in M_x$, where M_x is a compact set, the optimal parameter vector is defined as:*

$$\theta^* = \arg\min_{\hat{\theta} \in M_\theta}\left[\sup_{x \in M_x}\left\|\eta(x) - \hat{\eta}\left(x, \hat{\theta}\right)\right\|\right] \tag{15}$$

Assume that θ^* lies in a convex area M_θ, $M_\theta = \{\theta | \, \|\theta\| \leq m_\theta\}$, and m_θ is design parameter.

According to Assumption 2.3 and the universal approximation theorem of fuzzy system, we define

$$\eta = \hat{\eta}\left(x, \theta^*\right) + \kappa, \quad \|\kappa\| \leq \bar{\kappa} \tag{16}$$

where κ is approximation error, and $\bar{\kappa} > 0$ is the approximation error upper bound.

3. Control Design.

3.1. **Structure of a novel control scheme.** Figure 3 shows the structure of the proposed novel path following control scheme for the underactuated USV with external disturbances. First, for the system of underactuated model, a nonlinear coordinate transformation is constructed in this paper, which will result in a "global design". Then the second-order linear differentiator (SOLD) is introduced to realize the derivatives of the nominal states wherever it is needed, as well as to provide command filtering. Next, path following controller is designed by using TLC method, which consists of two parts:

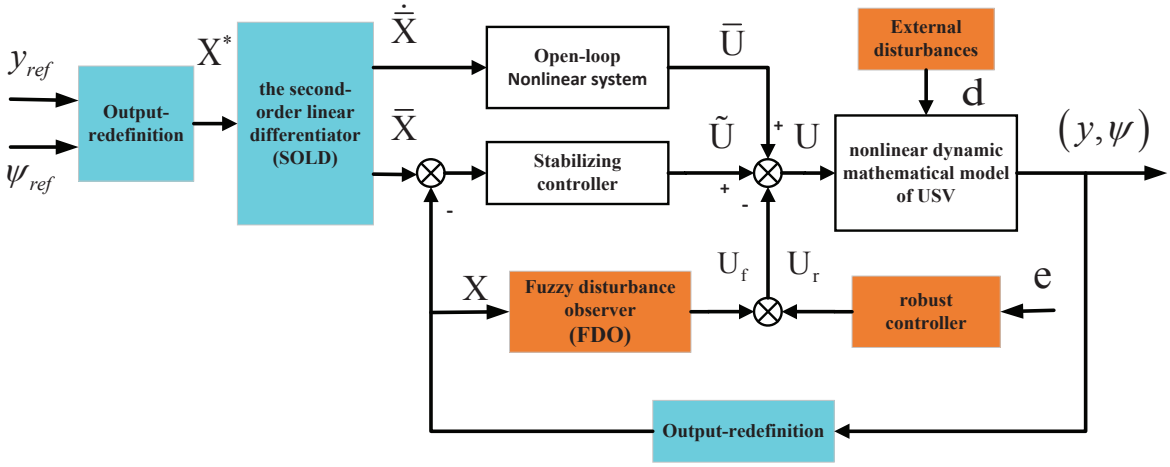

FIGURE 3. The structure of the proposed path following control scheme for the underactuated USV

the first part is pseudo-dynamic inverse controller $\bar{U}$ (open-loop control) which generates the nominal control input; the second part is a feedback controller $\tilde{U}$ (close-loop control) which stabilizes the system tracking error dynamics along the nominal trajectory. Finally, to enhance performance of the system, a FDO and robust control term are designed. The principle is that the output U_f of FDO compensates the influence of uncertain factor of the system, and robust control term U_r can overcome the influence of approximation error. In addition, the mathematical expression of the scheme is

$$U = \bar{U} + \tilde{U} - U_f - U_r \tag{17}$$

where $\bar{U}$ and $\tilde{U}$ are the output of TLC, and U_f and U_r are the output of FDO and robust control term, respectively.

3.2. **Output-redefinition.** Owing to that the system model of this paper has underactuated characteristics, the path following controller cannot be designed directly by TLC. Hence, we introduce the following coordinate transformation:

$$w_e = \psi + \arcsin\left(\frac{ky}{\sqrt{1+(ky)^2}}\right) \tag{18}$$

where w_e is output of the output-redefinition, and k is a positive constant to be selected later.

Remark 3.1. *The above coordinate transformation is well output-redefinition, where the function* arcsin *is not unique. Other functions can also be selected, such as* tanh, arctan, *which are smooth bounded functions. We can also choose linear coordinate transformation, such as* $w_e = \psi + ky$. *However, when* y *is large, it can result in USV whirling around [33].*

Theorem 3.1. *Subsystem (18), when* $w_e \to 0$, ψ *and* y *will converge to* 0*; conversely, when* $\psi \to 0$, $y \to 0$, *then* $w_e \to 0$.

Proof: According to subsystem (18), we can obtain

$$\psi = w_e - \arcsin\left(\frac{ky}{\sqrt{1+(ky)^2}}\right) \tag{19}$$

Substituting (19) into $\dot{y}$ of subsystem (4) satisfies

$$\dot{y} = U_n \sin\left(w_e - \arcsin\left(\frac{ky}{\sqrt{1+(ky)^2}}\right)\right) \tag{20}$$

When $w_e \to 0$, subsystem (20) can be simplified to

$$\dot{y} = -\frac{kU_n}{\sqrt{1+(ky)^2}} y \tag{21}$$

Considering the Lyapunov function candidate $V_y = \frac{1}{2}y^2$, we have

$$\dot{V}_y = y\dot{y} = -\frac{kU_n}{\sqrt{1+(ky)^2}} y^2 \leq 0 \tag{22}$$

It is obvious that $\dot{V}_y = 0$ only when $y = 0$. And from subsystem (18), when $y = 0$, ψ will always be equivalent to zero. Obviously, when $\psi \to 0$, $y \to 0$, and substituting into (18), then $w_e \to 0$. □

Upon application of the coordinate transformation (18), we obtain

$$\begin{cases} \dot{y} = U_n \left[\sin w_e \dfrac{1}{\sqrt{1+(ky)^2}} - \cos w_e \dfrac{ky}{\sqrt{1+(ky)^2}}\right] \\ \dot{w}_e = r + \dfrac{kU_n}{1+(ky)^2}\left[\sin w_e \dfrac{1}{\sqrt{1+(ky)^2}} - \cos w_e \dfrac{ky}{\sqrt{1+(ky)^2}}\right] \\ \dot{r} = -\dfrac{1}{T}r - \dfrac{\alpha}{T}r^3 + \dfrac{K}{T}\delta + \eta \\ s = w_e \end{cases} \tag{23}$$

Define $X = [x_1, x_2]^T = [w_e, r]^T$, $U = \delta$, $\lambda = U_n\left[\sin x_1 \frac{1}{\sqrt{1+(ky)^2}} - \cos x_1 \frac{ky}{\sqrt{1+(ky)^2}}\right]$. The derivative of y is λ, $f_1(X) = x_2 + \frac{k}{1+(ky)^2}\lambda$, $f_2(X) = -\frac{1}{T}x_2 - \frac{\alpha}{T}{x_2}^3$, $b = \frac{K}{T}$. In this paper, system (23) is transformed into an affine nonlinear equation, which can be expressed as

$$\begin{cases} \dot{X} = f(X) + g_1(X)U + \Theta(X)\eta \\ Y = x_1 \end{cases} \tag{24}$$

where $f(X) = [f_1(X), f_2(X)]^T$, $g_1(X) = [0, b]^T$, $\Theta(X) = [0, 1]^T$.

To sum up, when $w_e \to 0$, the systems (4) and (24) are equivalent. We obtain a novel control objective: w_e of system (24) converges to 0 through the design of the controller U.

3.3. **Trajectory linearization controller design.** In the TLC framework, it consists of two parts: the pseudo-dynamic inverse controller and the stabilizing controller. First, the pseudo-dynamic inverse controller is designed. In this paper, SOLD is applied to producing $\bar{X}$ and $\dot{\bar{X}}$ by the nominal input X^*, as well as to provide command filtering. Transfer function form of X^* to $\dot{\bar{X}}$ can be expressed as

$$w(s) = \frac{s}{T^2s^2 + 2Ts + 1} = \frac{s}{(Ts+1)^2} \tag{25}$$

where T is the time constant. From its transfer function form, the state-space form can be written as

$$\begin{cases} \dot{X}_1 = X_2 \\ T^2\dot{X}_2 = -\left(X_1 - X^*\right) - 2TX_2 \\ y = X_2 \end{cases} \tag{26}$$

It is obvious to know that $\lim_{T\to 0} X_1 = X^* = \bar{X}$, $\lim_{T\to 0} X_2 = \dot{X}^* = \dot{\bar{X}}$. Here, when uncertainties of the system are not considered, the control law is obtained by inverting (24)

$$\bar{U} = b^{-1}\left(\dot{\bar{X}} - f_2\left(\bar{X}\right)\right) \tag{27}$$

where $\bar{U}$ is nominal control law.

Then, the stabilizing controller is designed. From the design principle of TLC, define tracking error state variables $e = X - \bar{X}$. Linearizing (24) along the nominal trajectories $\left[\bar{X}, \bar{U}\right]^T$ yields

$$\dot{e} = A(t)e + B(t)\tilde{U} \tag{28}$$

where $A(t) = A\left(\bar{X}, \bar{U}\right) = \left(\frac{\partial f}{\partial X} + \frac{\partial g_1}{\partial X}U\right)\big|_{\bar{X},\bar{U}}$, $B(t) = B\left(\bar{X}, \bar{U}\right) = g_1\big|_{\bar{X},\bar{U}}$.

Assume (28) is strongly controllable. Defining a state transformation $e = L(t)z$, we transform (28) into a canonical form as

$$\dot{z} = A_z(t)z + B(t)\tilde{U} \tag{29}$$

where $A_z(t) = \begin{bmatrix} 0 & 1 \\ a_{21} & a_{22} \end{bmatrix}$, here $a_{21} = \left(\frac{1}{T} + \frac{3\alpha}{T}{x_2}^2\right)\frac{k}{1+(ky)^2}\lambda$, $a_{22} = \frac{k}{1+(ky)^2}\lambda - \frac{1}{T} - \frac{3\alpha}{T}{x_2}^2$.

From (10) and (11), the closed-loop tracking error dynamic can be written as

$$\dot{z} = A_c(t)z \tag{30}$$

where $A_c(t) = A_z(t) + B(t)K(t)$, $\tilde{U} = K(t)z$.

Assume that the desired closed-loop dynamics for (29) can be described as follows

$$\dot{z} = A_{cl}(t)z \tag{31}$$

with $A_{cl}(t) = \begin{bmatrix} 0 & 1 \\ -\tau_{j1} & -\tau_{j2} \end{bmatrix}$, where $\tau_{j1}(t) > 0$, $\tau_{j2}(t) > 0$ $(j = 1)$ can be gained from the close loop quadratic PD-eigenvalues. The PD-eigenvalues are chosen by specifying the desired closed-loop dynamics as

$$\begin{aligned} \tau_{j1}(t) &= \omega_{nj}^2(t) \\ \tau_{j2}(t) &= 2\zeta_j\omega_{nj}(t) - \frac{\dot{\omega}_{nj}(t)}{\omega_{nj}(t)} \end{aligned} \tag{32}$$

where ζ_j is the constant damping, $\omega_{nj}(t)$ is the constant damping. Then the stabilizing control law can be obtained as

$$\tilde{U} = K(t)L^{-1}(t)e \tag{33}$$

Finally, the total control law of the TLC is

$$U = \bar{U} + \tilde{U} \tag{34}$$

3.4. **FDO design.** When uncertainties of the system are considered, to enhance performance of the system, an FDO is designed to estimate the system uncertainties $\eta(X)$. Assume that there exists a nonlinear matrix $g_0(X)^{2\times 1}$, and it can satisfy the following matching conditions

$$\Theta(X) = g_0(X)g_1(X) \tag{35}$$

Considering uncertainties of the system, the system (8) can be expressed as

$$\dot{e} = F(t,e) + \Theta(X)\eta \tag{36}$$

From (35), substituting (17) into (36), we have

$$\dot{e} = F(t,e) + \Theta(X)\left(\eta - U_f - U_r\right) \tag{37}$$

where $U_f = g_0(X)\hat{\eta}$, $U_r = g_0(X)\nu$, $\hat{\eta}$ is estimate uncertainties of the system, and ν is robust control term, respectively.

Theorem 3.2. *Consider the following dynamic system*

$$\dot{\xi} = -\varepsilon\xi + \varphi\left(X,\hat{\theta}\right) \tag{38}$$

where $\varphi\left(X,\hat{\theta}\right) = \varepsilon X + f(X) + g_1(X)U + \Theta(X)\hat{\eta}\left(X,\hat{\theta}\right)$ *and* $\varepsilon > 0$ *is design parameter. Define the system uncertainties observation error as* $\chi = X - \xi$*, suppose there exists adjustable parameter vector* $\hat{\theta}$ *which is bounded, satisfying*

$$\dot{\hat{\theta}} = \beta\chi^T\Theta(X)\vartheta(X) - \Gamma_\theta\beta\frac{\chi^T\Theta(X)\hat{\theta}^T\vartheta(X)}{\left\|\hat{\theta}\right\|^2}\hat{\theta} \tag{39}$$

where $\Gamma_\theta = \begin{cases} 0, & \left\|\hat{\theta}\right\| < M_\theta,\ or\ \left\|\hat{\theta}\right\| = M_\theta,\ \chi^T\Theta(X)\hat{\theta}^T\vartheta(X) \geq 0 \\ 1, & \left\|\hat{\theta}\right\| = M_\theta,\ \chi^T\Theta(X)\hat{\theta}^T\vartheta(X) < 0 \end{cases}$ *and* β *is the learning rate. Then the system uncertainties observation error is uniformly ultimately bounded (UUB).*

Proof: From system (38) and the expression of $\varphi\left(X,\hat{\theta}\right)$, we obtain

$$\dot{\xi} = \varepsilon(X-\xi) + f(X) + g_1(X)U + \Theta(X)\hat{\eta}\left(X,\hat{\theta}\right) \tag{40}$$

Differentiating $\chi = X - \xi$, from (16) and (40), we have

$$\dot{\chi} = -\varepsilon\chi + \Theta(X)\left(\hat{\eta}\left(x,\theta^*\right) - \hat{\eta}\left(x,\hat{\theta}\right) + \kappa\right) \tag{41}$$

Define weight error $\tilde{\theta} = \theta^* - \hat{\theta}$, and (41) can be simplified as

$$\dot{\chi} = -\varepsilon\chi + \Theta(X)\left(\tilde{\theta}^T\vartheta(X) + \kappa\right) \tag{42}$$

The Lyapunov function candidate is given by

$$V_1 = \frac{1}{2}\chi^T\chi + \frac{1}{2\beta}\tilde{\theta}^T\tilde{\theta} \tag{43}$$

Differentiating (43) and substituting (42) into (43) yield

$$\dot{V}_1 = \chi^T\dot{\chi} + \frac{1}{\beta}\tilde{\theta}^T\dot{\tilde{\theta}} = -\varepsilon\chi^T\chi + \chi^T\Theta(X)\kappa + \frac{1}{\beta}\tilde{\theta}^T\left(\dot{\tilde{\theta}} + \beta\chi^T\Theta(X)\vartheta(X)\right) \tag{44}$$

Because $\dot{\tilde{\theta}} = -\dot{\hat{\theta}}$, substituting (39) into (44) yield

$$\dot{V}_1 \leq -\varepsilon\chi^T\chi + \chi^T\Theta(X)\kappa \tag{45}$$

Now, since $\|\kappa\| \leq \bar{\kappa}$, define $\bar{\kappa} = \Theta(X)\kappa$, we obtain

$$\|\bar{\kappa}\| = \|\Theta(X)\kappa\| \leq \|\Theta(X)\|\kappa \triangleq \bar{\kappa} \tag{46}$$

From (46), the system (45) can be simplified to

$$\dot{V}_1 \leq -\varepsilon\|\chi\|^2 + \chi^T\bar{\kappa} \leq -\varepsilon\|\chi\|^2 + \frac{\varepsilon}{2}\|\chi\|^2 + \frac{1}{2\varepsilon}\bar{\kappa}^2 \leq -\frac{\varepsilon}{2}\|\chi\|^2 + \frac{1}{2\varepsilon}\bar{\kappa}^2 \tag{47}$$

Thus, $\dot{V}_1$ is negative for $\|\chi\| > (\bar{\kappa}/\varepsilon)$. At this time, the system uncertainties observation error is UUB. □

Remark 3.2. *The proposed FDO method has two advantages in this paper. First, it has adaptive ability to estimate and compensate the system uncertainties. Then it guarantees the uniformly ultimately bounded of the disturbance observation error within a sufficiently small region by the appropriate choice of the design parameter ε.*

Although FDO has the ability to estimate and compensate the system uncertainties under the rate of parameter adjustment, the approximation error of the system is not considered. Therefore, to further improve the performance of the control system, robust control term is given as

$$\nu = \frac{\Xi}{\beta} \tag{48}$$

where $\Xi = \Theta^T(X)P(t)e$, and $P(t)$ is a symmetric matrix which satisfies Theorem 3.3.

Theorem 3.3. *Considering a linear time-varying system [27]*

$$\dot{X} = A_c(t)X \tag{49}$$

where $A_c(t)$ is continuous and bounded, and the origin is the only equilibrium state. Let $Q(t)$ be a continuous, bounded, positive definite, symmetric matrix, such that

$$0 < c_3 I \leq Q(t) \leq c_4 I \tag{50}$$

with I being a diagonal matrix. There exists a symmetric matrix $P(t)$ which satisfies a Lyapunov function

$$P(t)A_c(t) + A_c^T(t)P(t) + \dot{P}(t) + Q(t) = 0 \tag{51}$$

where $P(t)$ satisfies the following property

$$0 < c_1 I \leq P(t) \leq c_2 I \tag{52}$$

with $c_1, c_2 > 0$, $c_3, c_4 > 0$.

So far, the total design of path following control rate is

$$U = \bar{U} + \tilde{U} - g_0(X)\hat{\eta} - g_0(X)\nu \tag{53}$$

4. Stability Analysis.

Theorem 4.1. *Consider the following dynamic systems (24) and (38), define the system uncertainties observation error the same as Theorem 3.3, and the total design of control rate is (53). There exists adjustable parameter vector $\hat{\theta}$ of FDO as*

$$\dot{\hat{\theta}} = \beta\chi^T\Theta(X)\vartheta(X) + \beta\Xi^T\vartheta(X) - \Gamma_\theta\beta\frac{\chi^T\Theta(X)\hat{\theta}^T\vartheta(X) + \Xi^T\vartheta(X)}{\left\|\hat{\theta}\right\|^2}\hat{\theta} \tag{54}$$

where $\Gamma_\theta = \begin{cases} 0, & \left\|\hat{\theta}\right\| < M_\theta, \text{ or } \left\|\hat{\theta}\right\| = M_\theta, \left(\chi^T + \Xi^T\right)\Theta(X)\hat{\theta}^T\vartheta(X) \geq 0 \\ 1, & \left\|\hat{\theta}\right\| = M_\theta, \left(\chi^T + \Xi^T\right)\Theta(X)\hat{\theta}^T\vartheta(X) < 0 \end{cases}$. *Here, suppose we select $c_3 \geq 2c_2\ell\Psi$, where $\Psi < \min\{R_e, c_3/(2c_2\ell)\}$. In the case of control rate*

(53), the tracking error e and the system uncertainties observation error χ are uniformly ultimately bounded (UUB).

Proof: From Assumption 2.1, system (39) becomes (55) by Taylor expansion

$$\dot{e} = A(t)e + B(t)\tilde{U} + o(\bullet) + \Theta(X)\left(\eta - \hat{\eta} - \nu\right) \tag{55}$$

where $o(\bullet)$ means higher order terms of linearization, and $\|o(\bullet)\| \leq \ell\|e(t)\|^2$ is proposed in [27]. From (11), the system (55) can be written as

$$\dot{e} = A_c(t)e + o(\bullet) + \Theta(X)\left(\eta - \hat{\eta} - \nu\right) \tag{56}$$

The Lyapunov function candidate is given by

$$V = \frac{1}{2}e^T P e + \frac{1}{2\beta}\tilde{\theta}^T\tilde{\theta} + \frac{1}{2}\chi^T\chi \tag{57}$$

Differentiating (57) and substituting (42), (56) into (57) yield

$$\begin{aligned}\dot{V} = &\frac{1}{2}e^T\left(P(t)A_c(t) + A_c^T(t)P(t) + \dot{P}(t)\right)e + e^T P(t)o(\bullet) + \Xi^T\left(\eta - \hat{\eta} - \nu\right)\\ &+ \frac{1}{\beta}\tilde{\theta}^T\dot{\tilde{\theta}} + \chi^T\left(-\varepsilon\chi + \Theta(X)\left(\tilde{\theta}^T\vartheta(X) + \kappa\right)\right)\end{aligned} \tag{58}$$

From (16), (48) and (51), we have

$$\begin{aligned}\dot{V} = &-\frac{1}{2}e^T Q(t)e + e^T P(t)o(\bullet) - \Xi^T\frac{\Xi}{\beta} - \varepsilon\chi^T\chi + \chi^T\Theta(X)\kappa + \Xi^T\kappa\\ &+ \frac{1}{\beta}\tilde{\theta}^T\left(\dot{\tilde{\theta}} + \beta r^T\vartheta(X) + \beta\chi^T\Theta(X)\vartheta(X)\right)\end{aligned} \tag{59}$$

Because $\dot{\tilde{\theta}} = -\hat{\theta}$, substituting (50), (52), (54) into (59) yields

$$\dot{V} \leq -\frac{1}{2}c_3\|e\|^2 + c_2\ell\|e(t)\|^3 + \bar{\kappa}\|\Xi\| - \varepsilon\|\chi\|^2 + \bar{\kappa}\|\chi\| \tag{60}$$

From inequality, we have

$$\begin{aligned}\bar{\kappa}\|\Xi\| &\leq \frac{\bar{\kappa}^2}{2} + \frac{1}{2}\|\Xi\|^2\\ -\varepsilon\|\chi\|^2 + \bar{\kappa}\|\chi\| &\leq -\frac{\varepsilon}{2}\|\chi\|^2 + \frac{\bar{\kappa}^2}{2\varepsilon}\end{aligned} \tag{61}$$

From Theorem 4.1, any tracking error $\|e\| < \Psi$. Here define $\gamma = \bar{\kappa}^2 + \|\Xi\|^2 + \frac{\bar{\kappa}^2}{\varepsilon}$, and (60) can be simplified to

$$\begin{aligned}\dot{V} &\leq -\frac{1}{2}\left(c_3 - 2c_2\ell\Psi\right)\|e\|^2 - \frac{\varepsilon}{2}\|\chi\|^2 + \frac{1}{2}\|\Xi\|^2 + \frac{\bar{\kappa}}{2} + \frac{\bar{\kappa}^2}{2\varepsilon}\\ &\leq -\frac{1}{2}\left(c_3 - 2c_2\ell\Psi\right)\|e\|^2 - \frac{\varepsilon}{2}\|\chi\|^2 + \frac{1}{2}\gamma\end{aligned} \tag{62}$$

where $\dot{V} \leq 0$ for either $\|e\| > \sqrt{\gamma/(c_3 - 2c_2\ell\Psi)}$ or $\|\chi\| > \sqrt{\gamma/\varepsilon}$.

Thus, $\dot{V}$ is negative outside a compact set [23]. This demonstrates the UUB or both $\|e\|$ and $\|\chi\|$. For any initial error $\|e(t_0)\| < \min\{R_e, c_3/(2c_2\ell)\}$, the system uncertainties observation error and tracking error are UUB, where the tracking error converges to the ball $\|e\| \leq \sqrt{\gamma/(c_3 - 2c_2\ell\Psi)}$. □

5. **Simulation Results and Comparison.** To evaluate the effectiveness and performance of the proposed path following control scheme for the underactuated USV, we take Dalian Maritime University "LanXin" USV as the research object. Numerical simulations have been carried out based on the mathematical model described by (4). By using PD-spectrum theory [31,32], the control parameters of TLC are selected as $\zeta = 0.7$, $\omega_n = 3$. Define 7 fuzzy sets of x_j $(j = 1, 2)$, which are $A_j^1(NB)$, $A_j^2(NM)$, $A_j^3(NS)$, $A_j^4(ZE)$, $A_j^5(PS)$, $A_j^6(PM)$, $A_j^7(PB)$, respectively. The membership functions are selected as

$$u_{A_j}^i(x_j) = \exp\left\{-[x_j + 0.1(4-i)]^2\right\}, \quad i = 1, \ldots, 7 \tag{63}$$

where we use 49 rules of fuzzy systems to approximate the uncertainties of the system.

Here, by model identification in [34], the parameters of the underactuated USV are selected as $K = 0.707$, $T = 0.332$, $\alpha = 0.001$. The initial conditions of the underactuated USV are shown in Table 1.

TABLE 1. The initial parameters of USV

Initial condition	Value
$X(0)$	0
$Y(0)$	300 m
$\psi(0)$	0
$\mu(0)$	5 m/s
$v(0)$	0
$r(0)$	0

Other design parameters are selected as $k = 0.005$, $\varepsilon = 4$, $\beta = 1000$, $Q(t) = I_{2\times 2}$.

To show the results of comparison more clearly, an integration of time and absolute error (ITAE) performance evaluation index is employed to describe the output-redefintion w_e. The ITAE can be represented as

$$\text{ITAE} = \int_0^t t|e(t)|dt \tag{64}$$

In simulation study, the simulation results consist of two parts: the first part is control performance of the original TLC in three cases; the second part is to demonstrate the effectiveness of this paper proposed control strategy. The following three cases are considered in this paper [35].

Case 1. There exist no unmodeled dynamics and external disturbances.

Case 2. The unmodeled dynamics exist in the system described as

$$\eta = 0.2\sin(0.1t) \tag{65}$$

Case 3. Both unmodeled dynamics and external disturbances exist in the system described as

$$\eta = 0.2\sin(0.1t) + 0.3\sin(0.3t) \tag{66}$$

First, in order to prove control performance of the original TLC in the field of ship motion control, simulations of the TLC method have been carried out in three cases. The simulation results are shown in Figure 4.

From Figure 4, under Case 1, it can be observed that the USV can exhibit nice following property, course ψ and output-redefintion w_e results converge to zero, and rudder angle δ tends to a constant in a very short time, respectively. Under Cases 2 and 3, Figure 4(a) shows that the following performance of TLC degrades remarkably, and the simulation

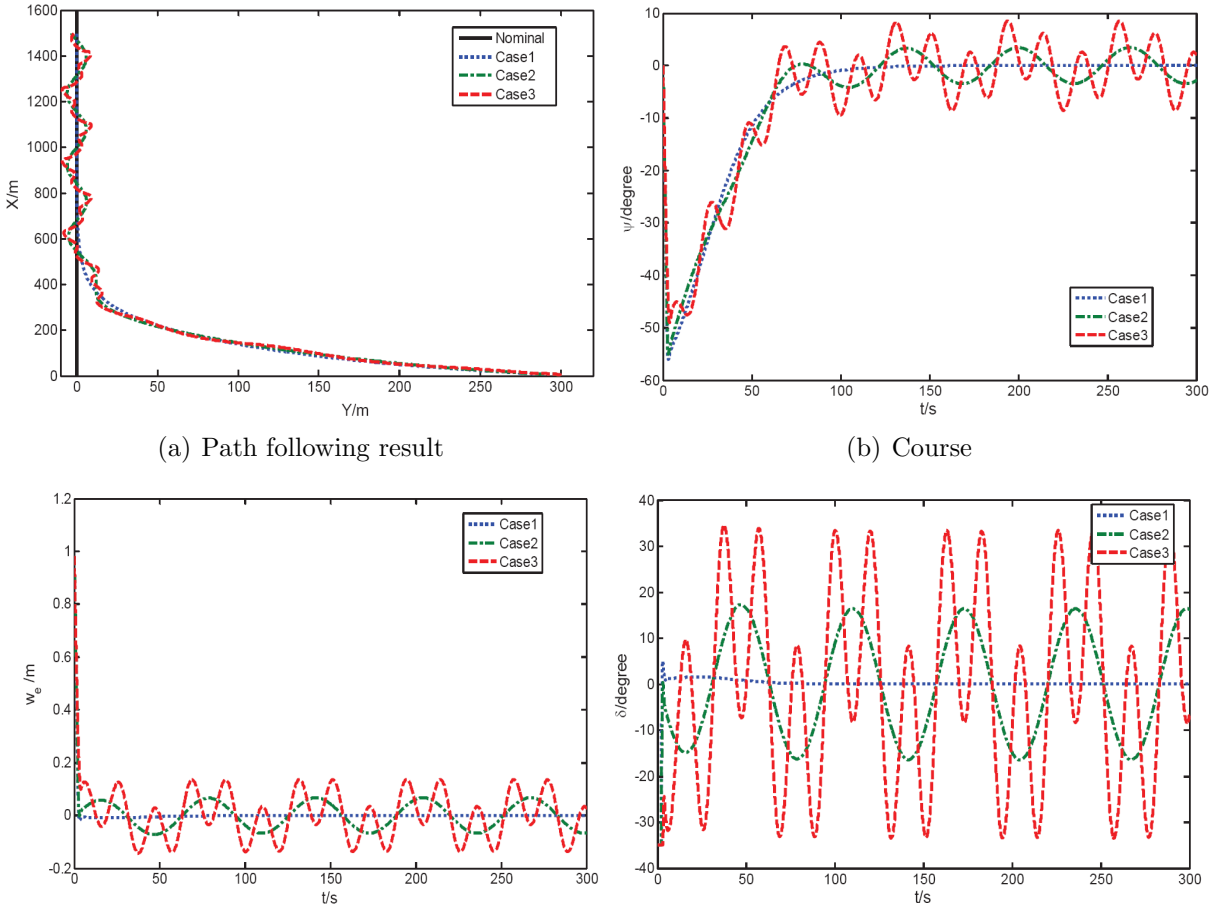

(a) Path following result

(b) Course

(c) Output-redefintion w_e

(d) Rudder angle

FIGURE 4. Simulation results of the TLC method

results have a large range of variation in Figures 4(b), 4(c) and 4(d). That is because the local exponential stability cannot make the TLC have enough anti-interference and robustness. Thus, with the increase uncertainties of the system, the performance of TLC cannot be ensured.

Second, simulations are carried out to verify the effectiveness of this paper proposed control strategy. For the purpose of comparison, the following two controllers are given as:

(1) TLC: This is an original TLC method in Figure 4;

(2) NDO-TLC: This is a controller combined with nonlinear disturbance observer (NDO) proposed in [36]. The difference is that the uncertainties of the system are estimated online through the NDO. The control parameters are selected as $\omega_n = 2$, $\zeta = 0.7$, $P(x) = x_2 + \frac{{x_2}^3}{3}$, $l(x) = 1 + {x_2}^2$.

Under Case 2, the comparison results can be shown in Figure 5.

From Figure 5(a), it can be observed that the USV tracks the reference straight-line path accurately under the FDO-TLC controller. Similarly, Figure 5(b) and Figure 5(c) show that course ψ and output-redefintion w_e results converge to zero in a very short time. However, the simulation results of TLC and NDO-TLC show that there is an oscillation in the equilibrium position. Because under the unmodeled dynamics, the control performance of TLC and NDO-TLC is poor. However, FDO-TLC can estimate the unmodeled error to achieve real-time online compensation, and robust control term can overcome the

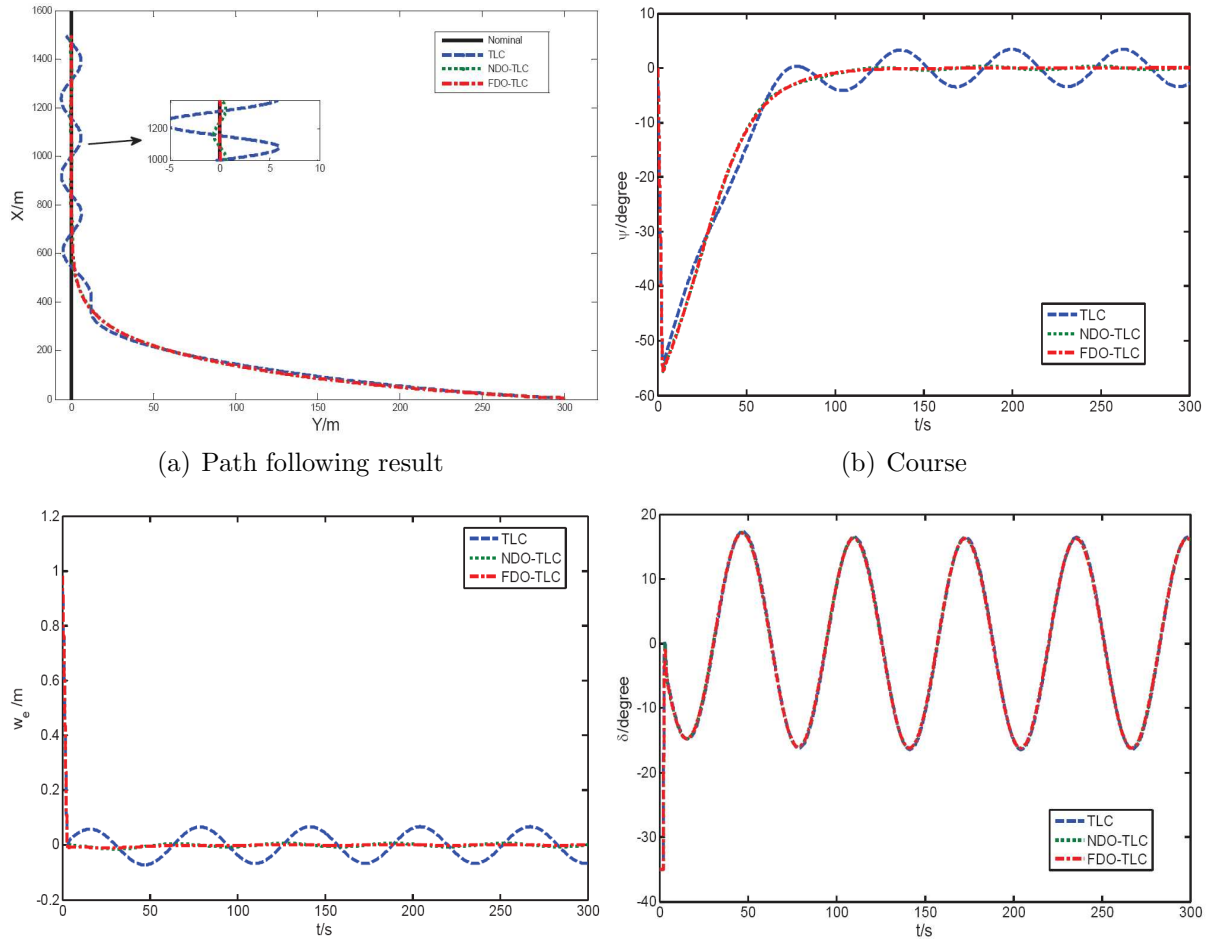

(a) Path following result

(b) Course

(c) Output-redefintion w_e

(d) Rudder angle

FIGURE 5. Simulation results under Case 2

influence of approximation error. Thus, the stability of the whole system is improved, and the control performance of FDO-TLC is the best in the comparison.

Under Case 3, the comparison results can be shown in Figure 6.

In Figure 6, compared with TLC and NDO-TLC, FDO-TLC still has good control effect. Although NDO-TLC can estimate uncertainties of the system and compensate for it, the estimation ability will be significantly decreased with the increase uncertainties of the system. However, FDO-TLC can be capable of online estimating through adaptive parameter learning, and the estimation ability will change with the change of external disturbances. Therefore, FDO-TLC has better control performance.

In three cases, the ITAE index of the output-redefintion w_e is shown in Table 2.

As can be seen from Table 2, the ITAE value of FDO-TLC is the smallest in three cases. With the increase uncertainties of the system, the range of change is also the smallest. Thus, the control performance of FDO-TLC is the best in the comparison.

From what is said above, it can be found clearly that the underactuated USV tracks the reference straight-line path accurately under FDO-TLC control. The simulation results indicate the correctness and effectiveness for the proposed path following control scheme.

6. **Conclusions.** In this paper, a novel path following control scheme combined with the advantages of TLC and FDO is developed to address tracking problem of the underactuated USV. First, output-redefinition is introduced to solve the underactuated model

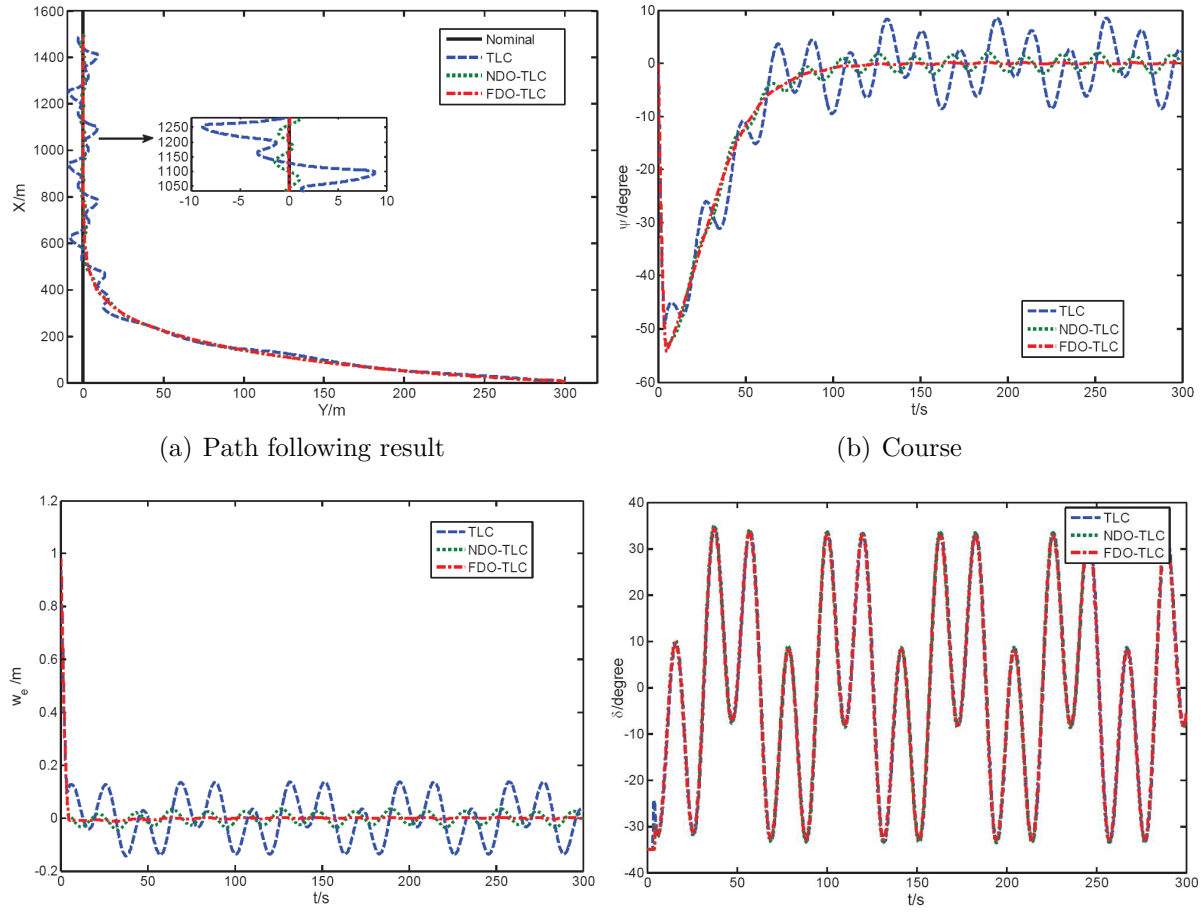

(a) Path following result

(b) Course

(c) Output-redefintion w_e

(d) Rudder angle

FIGURE 6. Simulation results under Case 3

TABLE 2. The ITAE index of the output-redefintion w_e

	TLC	NDO-TLC	FDO-TLC
Case 1	16.82	16.82	16.82
Case 2	1934	197.9	31.47
Case 3	3251	845	86.02

problems. Then by using TLC method, a path following controller is designed. However, the performance of TLC will be significantly decreased with the increase uncertainties of the system. Therefore, to enhance performance of the system, FDO is constructed in this paper, which can be capable of online estimating uncertainties of the system through parameter learning and compensating for it. Meanwhile, robust control term is designed to overcome the influence of approximation error. The stability of the closed-loop system is proved by Lyapunov functions. Finally, compared with TLC and NDO-TLC, the simulation results demonstrate the correctness of the proposed path following control scheme for the underactuated USV.

TLC is applied to the field of ship motion control, but it needs further improvement. In this paper, we have realized that the underactuated USV tracks the reference straight-line path accurately by FDO-TLC controller. Next, we will design a curve path following controller for the underactuated USV in a complex environment.

Acknowledgment. This work was partially supported by "the Nature Science Foundation of China" (grand number 51609033), "the Nature Science Foundation of Liaoning Province of China" (grand number 2015020022), and "the Fundamental Research Funds for the Central Universities" (grand numbers 3132014321, 3132016312 and 3132017133).

REFERENCES

[1] A. J. Sinisterra, M. R. Dhanak and K. V. Ellenrieder, Stereovision-based target tracking system for USV operations, *Ocean Engineering*, vol.133, pp.197-214, 2017.

[2] P. Encarnacao and A. Pascoal, Combined trajectory tracking and path following: An application to the coordinated control of autonomous marine craft, *IEEE Conference on Decision & Control*, vol.1, pp.964-969, 2002.

[3] Z. Cao, Y. Zhao and S. Wang, Trajectory tracking and point stabilization of noholonomic mobile robot, *IEEE/RS*, pp.1328-1333, 2010.

[4] D. D. Mu, G. F. Wang and Y. S. Fan, Design of adaptive neural tracking controller for pod propulsion unmanned vessel subject to unknown dynamics, *Journal of Electrical Engineering & Technology*, vol.12, no.6, pp.2365-2377, 2017.

[5] D. D. Mu, G. F. Wang, Y. S. Fan, X. J. Sun and B. B. Qiu, Adaptive LOS path following for a podded propulsion unmanned surface vehicle with uncertainty of model and actuator saturation, *Applied Sciences*, vol.7, no.12, 2017.

[6] M. Breivik and T. I. Fossen, Guidance-based path following for autonomous underwater vehicles, *Proc. of OCEANS 2005 MTS/IEEE*, vol.3, pp.2807-2814, 2005.

[7] Z. P. Jiang, Brief global tracking control of underactuated ships by Lyapunov's direct method, *Automatica*, vol.38, no.2, pp.301-309, 2002.

[8] Z. Zhao, W. He and S. S. Ge, Adaptive neural network control of a fully actuated marine surface vessel with multiple output constraints, *IEEE Trans. Control Systems Technology*, vol.22, no.4, pp.1536-1543, 2014.

[9] J. Shin, J. K. Dong and Y. I. Lee, Adaptive path-following control for an unmanned surface vessel using an identified dynamic model, *IEEE/ASME Trans. Mechatronics*, vol.22, no.3, pp.1143-1153, 2017.

[10] P. Wang and Z. Geng, Adaptive distributed dynamic surface control for cooperative path following of multi-robot systems with unknown uncertainties under directed graphs, *International Journal of Innovative Computing, Information and Control*, vol.13, no.1, pp.261-276, 2017.

[11] W. Naeem, T. Xu, R. Sutton and A. Tiano, The design of a navigation, guidance, and control system for an unmanned surface vehicle for environmental monitoring, *Proc. of the Institution of Mechanical Engineers, Part M – Journal of Engineering for the Maritime Environment*, vol.222, no.2, pp.67-79, 2008.

[12] H. Ashrafiuon, K. R Muske, L. C. Mcninch and R. A. Soltan, Sliding-mode tracking control of surface vessels, *IEEE Trans. Industrial Electronics*, vol.55, no.11, pp.4004-4012, 2008.

[13] L. C. Mcninch and H. Ashrafiuon, Predictive and sliding mode cascade control for unmanned surface vessels, *American Control Conference*, vol.145, no.2, pp.184-189, 2011.

[14] D. D. Mu, G. F. Wang, Y. S. Fan, Y. M. Bai and Y. S. Zhao, Fuzzy-based optimal adaptive line-of-sight path following for underactuated unmanned surface vehicle with uncertainties and time-varying disturbances, *Mathematical Problems in Engineering*, vol.6, pp.1-12, 2018.

[15] C. Liu, Z.-J. Zou and J.-C. Yin, Path following and stabilization of underactuated surface vessels based on adaptive hierarchical sliding mode, *International Journal of Innovative Computing, Information and Control*, vol.10, no.3, pp.909-918, 2014.

[16] Y. Yang, J. Du, H. Liu, C. Guo and A. Abraham, A trajectory tracking robust controller of surface vessels with disturbance uncertainties, *IEEE Trans. Control Systems Technology*, vol.22, no.4, pp.1511-1518, 2014.

[17] G. Zhang, X. Zhang and Y. Zheng, Adaptive neural path-following control for underactuated ships in fields of marine practice, *Ocean Engineering*, vol.104, pp.558-567, 2015.

[18] M. C. Mickle and J. J. Zhu, Skid to turn control of the APKWS missile using trajectory linearization technique, *American Control Conference*, vol.5, pp.3346-3351, 2001.

[19] J. Zhu, B. Banker and C. Hall, X-33 ascent flight control design by trajectory linearization – A singular perturbation approach, *Proc. of the AIAA Guidance, Navigation, and Control Conference*, 2006.

[20] B. Zhu and W. Huo, Adaptive trajectory linearization control for a model-scaled helicopter with uncertain inertial parameters, *Proc. of the 31st Chinese Control Conference*, pp.4389-4395, 2012.
[21] T. M. Adami and J. J. Zhu, 6DOF flight control of fixed-wing aircraft by trajectory linearization, *American Control Conference*, pp.1610-1617, 2011.
[22] Y. Liu and J. J. Zhu, Regular perturbation analysis for trajectory linearization control, *Proc. of the American Control Conference*, pp.3053-3058, 2007.
[23] Y. Liu, R. Huang and J. Zhu, Adaptive neural network control based on trajectory linearization control, *Proc. of the World Congress on Intelligent Control & Automation*, vol.1, pp.417-421, 2006.
[24] X. L. Shao and H. L. Wang, Back-stepping robust trajectory linearization control for hypersonic reentry vehicle via novel tracking differentiator, *Journal of the Franklin Institute*, vol.253, no.9, pp.1957-1984, 2016.
[25] X. L. Shao and H. L. Wang, Trajectory linearization control based output tracking method for nonlinear uncertain system using linear extended state observer, *Asian Journal of Control*, vol.18, no.1, pp.316-327, 2016.
[26] Y. Hu, H. Wang and Z. Ren, Adaptive trajectory linearization control for hypersonic reentry vehicle, *Journal of Central South University*, vol.23, no.11, pp.2876-2882, 2016.
[27] X. J. Zeng and M. G. Singh, Approximation theory of fuzzy systems – SISO case, *IEEE Trans. Fuzzy Systems*, vol.2, no.2, pp.162-176, 1994.
[28] X. L. Jia and Y. S. Yang, *Mathematical Model of Ship Motion*, Dalian Maritime University Press, Dalian, China, 1999.
[29] D. P. Li, *Ship Motion and Modeling*, National Defense Industry Press, Beijing, China, 2008.
[30] H. K. KHALIL, *Nonlinear Systems*, Prentice Hall, New York, America, 1996.
[31] M. C. Mickle and J. J. Zhu, Nonlinear missile planar autopilot design based on PD-spectrum assignment, *IEEE Conference on Decision & Control*, vol.4, pp.3914-3919, 1997.
[32] J. J. Zhu, PD-spectral theory for multivariable linear time-varying systems, *IEEE Conference on Decision & Control*, vol.4, pp.3908-3913, 1997.
[33] K. D. Do and J. Pan, State- and output-feedback robust path-following controllers for underactuated ships using Serret-Frenet frame, *Ocean Engineering*, vol.31, nos.5-6, pp.587-613, 2004.
[34] D. D. Mu, G. F. Wang, Y. S. Fan, Y. M. Bai and Y. S. Zhao, Path following for podded propulsion unmanned surface vehicle: Theory, simulation and experiment, *IEEJ Trans. Electrical & Electronic Engineering*, vol.137, no.1, pp.1-13, 2017.
[35] X. Shao and H. Wang, Active disturbance rejection based trajectory linearization control for hypersonic reentry vehicle with bounded uncertainties, *ISA Transactions*, vol.54, pp.27-38, 2015.
[36] L. Zhu, C. S. Jiang and W. Fang, Robust trajectory linearization control for uncertain nonlinear systems based on nonlinear disturbance observer, *Information & Control*, vol.35, no.6, pp.705-710, 2006.